

Range Safety Assessment Tool (RSAT): An analysis environment for safety assessment of launch and reentry vehicles

Francisco M. Capristan* and Juan J. Alonso †
Stanford University, Stanford, CA 94305, U.S.A.

The expected diversity in the kinds of vehicles that are currently appearing in the commercial space transportation sector raises questions about the possibility of improvements to current methodologies for licensing launch and reentry operations in use by the Federal Aviation Administration (FAA). These licensing procedures are designed to limit risks to public health and safety to acceptable levels and have served us well until now. Concerns may arise because the majority of methods in use are derived from expendable launch vehicles (ELVs) and the space shuttle era, and the possibility exists that they may be overly conservative. To investigate the extent to which the current methodology may be improved, an open source analysis environment for assessing the safety of the uninformed public on the ground has been developed. The safety analysis environment is called Range Safety Assessment Tool (RSAT), it can be used for launch and reentry operations and, in principle, can be applied for all kinds of vehicle configurations that may be proposed. RSAT uses random sampling techniques to calculate statistics of interest associated with ground risks due to vehicle malfunctions. The risks being modeled include inert and explosive debris effects, debris toxic gas dispersion, and blast overpressure due to vehicle explosions. Special consideration is given to quantifying the risk to the uninformed public by computing the appropriate safety metrics, which in this case is the value of the expected casualty per mission (E_{TC}). As part of this analysis environment, a 3-degree-of-freedom (DOF) trajectory optimization tool that uses a pseudospectral collocation method has been developed and is used to establish nominal trajectories for a number of different kinds of missions. In this paper, we present RSAT's major components and characteristics, and its predictive capabilities to analyze realistic launch and reentry accident scenarios. The output of the environment is verified and validated with existing data and previous calculations done with existing tools.

I. Introduction

One of the missions of the FAA Office of Commercial Space Transportation (AST) is to protect public health and safety during commercial launch and reentry activities.¹ To serve this purpose, the FAA requires candidate organizations to satisfy several requirements before it will issue a license for launch and reentry operations. For instance, candidates are required to demonstrate detailed trajectory analysis, debris risk analysis, flight hazard area analysis, and far-field overpressure effect analysis.² Most of these requirements are conservative and leveraged from lessons learned from expendable launch vehicles and the Space Shuttle era, and thus they might not be fully applicable to future vehicles, which might include suborbital vehicles, reusable launch vehicles (RLVs), and a number of hybrid configurations already on the drawing board.

Throughout the years, there have been a number of analysis tools developed to assess the risk associated with the launch or reentry of space vehicles. One of these tools is the Launch Risk Analysis (LARA), which was developed with the launch of missile and space boosters in mind.³ A more recent environment available for use by the industry is the Common Real-Time Footprint (CRTF),⁴ which provides probabilistic based debris footprints. For blast overpressure analysis there is the Distant Focusing Overpressure software

*PhD Candidate, Department of Aeronautics and Astronautics, Stanford University, Stanford, CA.

†Associate Professor, Department of Aeronautics & Astronautics, AIAA Associate Fellow.

(BlastDFO), which computes the risk due to blast waves resulting from a large near-pad explosion.⁵ There are other analysis tools that can perform the required safety analysis for licensing purposes. However, most of these analysis environments are proprietary and are neither available for academic research nor can their source code be obtained. This fact, added to the desire by the FAA AST to have access to an open source safety analysis environment that could be used as an independent analysis tool, motivates the development of an open source safety assessment environment that is based on tools of the necessary fidelity.

The safety analysis environment developed in this paper, RSAT, models risks to the uninjured public on the ground. It models risk effects due to inert falling debris, blast overpressure, explosive debris, and lethal gas dispersion from burning debris. The safety metric used to quantify these risks is E_{TC} , which is defined as the expected average number of human casualties per commercial space mission. A human casualty is defined as a fatality or serious injury.⁶ The current accepted maximum value for E_{TC} used by the FAA for licensing purposes is 30×10^{-6} casualties per mission (30 casualties per million missions).⁶ The environment considers uncertainties due to off nominal trajectories, atmospheric conditions, and breakup characteristics.

RSAT is written in Python with some modules written in Fortran and C++. The main advantage of using Python is that it allows flexibility in swapping modules in and out of the environment as appropriate for the scenario being investigated. Python is an interpreted language, but it allows us to add compiled components from other languages. In this paper, we focus on validating and understanding the results of RSAT so that it can be confidently used.

II. Analysis Environment

A sketch of RSAT is depicted in Figure 1. Uncertainties in the trajectory state vector, wind magnitude and direction, failure probability, and the number of debris pieces due to a breakup are some of the parameters that need to be modeled in order to obtain meaningful E_{TC} results. The vehicle state vector is used to set up the initial conditions for safety modeling. The state vectors at different times could be provided as inputs, or they could be generated for a specific mission given the vehicle characteristics. For this purpose, we have implemented a 3 DOF trajectory optimizer, the Stanford Program to Optimize Trajectories (SPOT), which can be used to obtain reasonable trajectory state vectors.

In case of vehicle breakup, a critical input for the analysis environment is the vehicle debris catalog, which is usually provided to the FAA as part of the licensing process. These catalogs contain information about the vehicle debris characteristics such as ballistic coefficient, number of pieces, aerodynamic characteristics, impulse velocity, etc. Debris catalogs are often grouped by ballistic coefficient, allowing debris pieces within a group to share some common aerodynamic characteristics. Generation of debris catalogs poses a challenging problem due to the highly nondeterministic characteristics of midair vehicle breakup. Furthermore, debris catalog generation requires detailed vehicle information.

Although the trajectory optimization algorithm within SPOT does not consider atmospheric uncertainties, the analysis environment does. In particular, the analysis environment can handle wind and density variations. In order to model atmospheric variations, we use the Earth Global Reference Atmospheric Model (Earth-GRAM 2010) developed at NASA. Earth-GRAM uses an empirical database that includes winds and other atmospheric parameters as a function of geographic position and time of the year. It provides the environment with density, temperature, pressure winds, and selected atmospheric constituent concentrations, from the surface of the Earth to orbital altitudes.⁷

E_{TC} calculations require information about the population density in the areas at risk. For reentry cases, the risk area could cover multiple continents; thus a population density map that covers all populated areas in the world is necessary. We use the Gridded Population of the World (GPW) which depicts the distribution of human population across the globe. GPW provides gridded population data that is constructed from national or subnational input units of varying resolution.⁸

The analysis environment considers people in different sheltering categories for calculating E_{TC} due to inert debris impacts. These categories correspond to the type of building structures protecting people. Census and economic statistics information are usually used to allocate the percentage of people in different sheltering categories. The sheltering methodology includes wood, tile, light metal, composite, steel, and concrete roof penetration models. By taking into consideration the time of the day and the economic statistics, the percentage of people in each sheltering category is calculated. By using the population density obtained from GPW, the number of people in each sheltering category is assigned. The sheltering model implemented in the analysis environment was suggested by Larson.⁹

To calculate E_{TC} , we define E_c as the expected number of casualties due to a particular catastrophic event. It could be a function of time or state vector. E_{TC} also requires knowledge of the failure rate (λ). An intermediate parameter, $E_{c_{rate}}$, is defined by

$$E_{c_{rate}} = \lambda E_c, \quad (1)$$

and the total expected casualty is calculated by

$$E_{TC} = \int_{t_0}^{t_f} E_{c_{rate}}(t) dt, \quad (2)$$

where t_0 and t_f represent the beginning and the end of the launch or reentry operations.

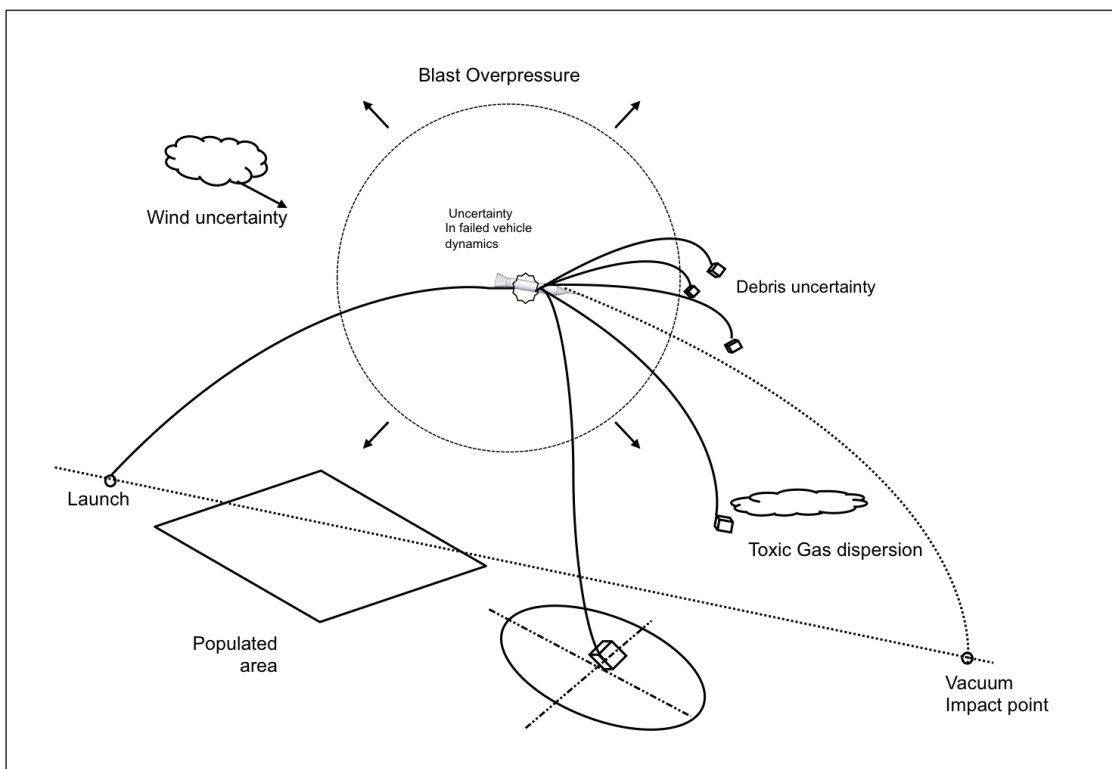


Figure 1: Safety Analysis Environment Representation

A. Trajectory Optimization

To obtain vehicle state vectors at different times during a trajectory we have developed SPOT. It uses a Chebyshev pseudospectral collocation method due to its large radius of convergence.¹⁰ The trajectory problem is formulated as a continuous time control problem in which the state and control variables are parameterized using global polynomials.¹¹ The problem is discretized to an orthogonal polynomial pseudospectral method requiring a non-uniform distribution, thus making the continuous time control problem a nonlinear programming problem (NLP).

In order to discretize time and differentiate the state vectors, consider the expression for time and the differentiation matrix for $N + 1$ nodes from the Chebyshev pseudospectral method,

$$tt_k = \cos(\pi k/N), \quad k=0, \dots, N \quad (3)$$

$$c_j = \begin{cases} 2 & \text{if } j = 0, N \\ 1 & 1 \leq j \leq N-1 \end{cases} \quad (4)$$

$$\mathbf{D}_{or} := [D_{or_{kj}}] = \begin{cases} (c_k/c_j)[(-1)^{j+k}/(tt_k - tt_j), & j \neq k \\ -tt_k/2(1 - tt_k^2), & 1 \leq j = k \leq N-1 \\ (2N^2 + 1)/6, & j = k = 0 \\ -(2N^2 + 1)/6, & j = k = N \end{cases} \quad (5)$$

Note that tt_k is in descending order and lies in the interval $[-1,1]$. In SPOT the non-dimensional time vector is in ascending order and lies in the interval $[0,1]$. By rescaling the parameters in the equations above, we get

$$t_k = \frac{1}{2}(1 - tt_k) \quad k=0, \dots, N \quad (6)$$

$$\mathbf{D} = -2\mathbf{D}_{or}, \quad (7)$$

where t_k is the non-dimensional time vector and \mathbf{D} is the new differentiation matrix.¹² The state equations are then discretized and non-dimensionalized at every node. The unknowns are the values of the controls and the states at these nodes. The control values are the thrust magnitude and direction. By using the choice of node points and the properties of Lagrange polynomials, the state equations are transformed into algebraic equations. The equations of motion are imposed as constraints at the nodes. The differentiation matrix is used to calculate the time derivatives of the position vector (velocity and acceleration). The equation of motions are shown below

$${}^{eci}\vec{v}_v = \frac{{}^{eci}\partial\vec{r}_v}{\partial t} \quad (8)$$

$${}^{eci}\vec{a}_v = \frac{\partial {}^{eci}\vec{v}_v}{\partial t} = \frac{1}{m_v}(F_T\vec{u} + \vec{F}_a + \vec{W}_v), \quad (9)$$

$$\frac{\partial m_v}{\partial t} = -\frac{F_T}{I_{sp}g_0} \quad (10)$$

where \vec{r}_v , ${}^{eci}\vec{v}_v$, ${}^{eci}\vec{a}_v$ are the position, velocity, and acceleration vectors of the vehicle in the Earth-centered inertial (ECI) coordinate frame. The thrust magnitude is given by F_T and the direction vector by \vec{u} . The sum of all aerodynamic forces (lift and drag) is given by \vec{F}_a . The weight of the vehicle is given by \vec{W}_v . The mass of the vehicle, specific impulse, and the gravity acceleration at Earth's surface is given by m_v , I_{sp} , and g_0 respectively. Equations 8-10 are imposed as constraints for the optimizer. The resulting NLP is then solved by using SNOPT¹³ or IPOPT¹⁴, optimization packages, which attempt to satisfy the Karush-Kuhn-Tucker (KKT) conditions.¹⁵ The objective function selected for ascent trajectories in SPOT is to minimize the propellant mass required to reach the desired orbit.

B. Debris Propagation

The debris propagation module is one of the most important components of the safety assessment tool, mainly because its outputs serve as inputs for the gas dispersion, and explosive debris modules. The debris trajectory is modeled with a 3DOF trajectory propagator written in Fortran and compiled as a Python module. The trajectory propagator includes atmospheric effects and it models a spherical or oblate Earth. The trajectory propagation equations are solved in the ECI frame and are similar to Equations 8-9. Lift and drag coefficients (C_L and C_D) are considered to be functions of the freestream mach number. The freestream velocity is given by:

$$\vec{v}_\infty = -({}^{eci}\vec{v}_d - \vec{v}_{wind} - \vec{v}_\oplus), \quad (11)$$

where the debris inertial velocity ${}^{eci}\vec{v}_d$, the wind velocity \vec{v}_{wind} , and the Earth's atmosphere velocity \vec{v}_\oplus are all expressed in the ECI frame. The drag and lift vectors are calculated by:

$$\vec{D} = \frac{1}{2} C_D \rho_\infty S_{ref} \|\vec{v}_\infty\| \vec{v}_\infty, \quad (12)$$

$$\vec{L} = \frac{1}{2} C_L \rho_\infty S_{ref} \|\vec{v}_\infty\|^2 \frac{(\vec{v}_\infty \times \vec{r}_d) \times (\vec{v}_\infty)}{\|(\vec{v}_\infty \times \vec{r}_d) \times (\vec{v}_\infty)\|}, \quad (13)$$

where the atmospheric density ρ_∞ can be obtained by using Earth-GRAM or assuming an exponential density model. The reference area S_{ref} is an input from the debris catalogs. The debris position vector \vec{r}_d is simply used to define the lift direction for our 3 DOF propagation model. Finally the acceleration vector in the ECI frame is computed by:

$${}^{eci} \vec{a}_d = \frac{\partial {}^{eci} \vec{v}_d}{\partial t} = \frac{1}{m_d} (\vec{L} + \vec{W} + \vec{D}), \quad (14)$$

where \vec{W} is the debris weight vector and m_d is the mass of the debris piece.

The debris propagation stops when the debris impacts the ground or reaches orbit. Hundreds of debris pieces from a debris group are initialized using Monte Carlo sampling and then propagated forward in time by the solver. The impact location (latitude and longitude) for each piece of debris is used to create a probability density function of ground impact location for a debris group.

1. Probability Density Function Formulation

The probability density formulations implemented in RSAT are a bivariate normal distribution and a kernel density estimation (KDE) with gaussian kernels. The bivariate normal distribution tends to be an acceptable model for impact probability when all dispersion sources are statically combined to get the overall impact distribution.¹⁶

First we define the vector containing the impact location for piece i by:

$$X_i = [lat_i \ lon_i]^T, \quad (15)$$

where lat and lon represent the latitude and longitude of impact. The average impact location estimate is:

$$\bar{X} = \frac{1}{n} \sum_{i=1}^n X_i, \quad (16)$$

where n is the number of debris samples. The covariance matrix estimate is given by:

$$S = \frac{1}{n-1} \sum_{i=1}^n (X_i - \bar{X})(X_i - \bar{X})^T, \quad (17)$$

the probability density function for a bivariate normal distribution is given by:

$$\hat{f}(\vec{x}) = \frac{1}{2\pi \sqrt{\det(S)}} e^{-\frac{1}{2}(\vec{x}-\bar{X})^T S^{-1}(\vec{x}-\bar{X})}. \quad (18)$$

For cases where the impact locations are not symmetric, the bivariate normal assumption does not provide accurate results. Therefore a non-parametric approach is taken for these cases. Non-parametric methods do not assume the form of the distribution. In range safety environments, a common non-parametric method used is the KDE. Many different kernel options are available, but gaussian kernels are the most popular and provide smooth probability densities. We have implemented a KDE methodology for range safety that uses gaussian kernels (based on work by Glonek et al.¹⁷). First, the eigenvalues and eigenvectors of the covariance matrix (Equation 17) are calculated:

$$\begin{pmatrix} S_1 & 0 \\ 0 & S_2 \end{pmatrix} = U^{-1} S U \quad (19)$$

$$U = \begin{pmatrix} s_x & -s_y \\ s_y & s_x \end{pmatrix}. \quad (20)$$

Then, we select the principal axis as the new coordinate system:

$$[P_i \ Q_i] = X_i^T U. \quad (21)$$

The bandwidth for P and Q can be expressed as

$$h = 1.06 \times \left(\min \left[\sigma, \frac{IQR}{1.34} \right] \right) n^{-1/5}, \quad (22)$$

where the standard deviation σ and the interquartile range (IQR) for P and Q are calculated independently. The bandwidth matrix combines the bandwidth parameters by:

$$H_2 = U \begin{pmatrix} h_1^2 & 0 \\ 0 & h_2^2 \end{pmatrix} U^{-1}, \quad (23)$$

finally, the probability density function is calculated by:

$$\hat{f}(\vec{x}) = \frac{1}{2\pi n \sqrt{\det(H_2)}} \sum_{i=1}^n e^{-\frac{1}{2}(\vec{x}-X_i)^T H_2^{-1}(\vec{x}-X_i)} \quad (24)$$

The selection of the bandwidth parameter is critical for KDE. Note that in the probability density function method above we are assuming that the variables in the principal axis coordinate frame (P and Q) are not correlated. In most cases this assumption is valid when the downrange of the debris impacts is small; thus it is not heavily affected by the Earth's curvature. Figure 2 illustrates a case where the debris downrange is large. It can be seen that the KDE formulation does not capture the impact location appropriately at the extremes of the impact locations.

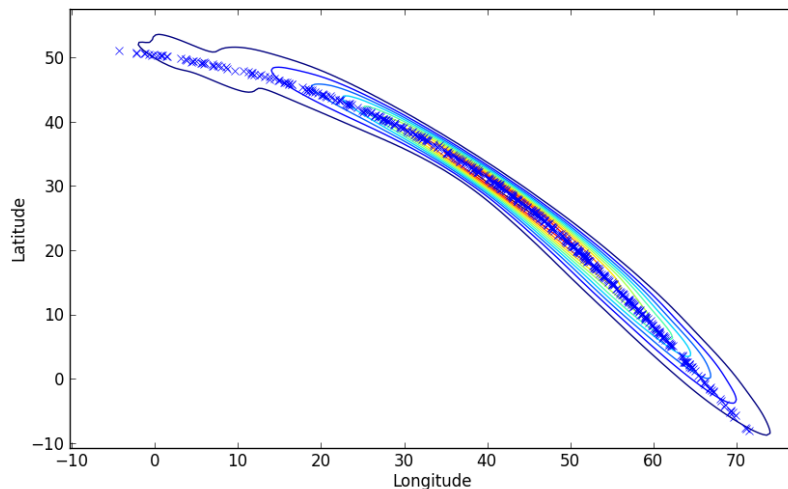


Figure 2: KDE Result

For failures near orbit insertion or reentry, the above formulation cannot be applied due to the large downrange generated by high speed pieces of debris impacting the ground. We propose an extra coordinate transformation that realigns the latitude and longitude impact locations such that they are almost uncorrelated. Let's consider a spherical Earth, such that:

$${}^{eccef} \vec{r}_i = \begin{pmatrix} \cos(lat_i) \cos(lon_i) \\ \cos(lat_i) \sin(lon_i) \\ \sin(lat_i) \end{pmatrix} \quad (25)$$

where ${}^{eccef} \vec{r}_i$ is the impact location unit vector in Earth Centered, Earth Fixed (ECEF) frame. Consider the mean impact location as

$${}^{ecef}\bar{\vec{r}} = \frac{1}{n} \sum_{i=1}^n {}^{ecef}\vec{r}_i, \quad (26)$$

which can be normalized to be a unit vector. Consider a new frame w given by:

$$R_{lon} = \begin{pmatrix} \cos(\overline{lon}) & \sin(\overline{lon}) & 0 \\ -\sin(\overline{lon}) & \cos(\overline{lon}) & 0 \\ 0 & 0 & 1 \end{pmatrix} \quad (27)$$

$$R_{lat} = \begin{pmatrix} \cos(\overline{lat}) & 0 & \sin(\overline{lat}) \\ 0 & 1 & 0 \\ -\sin(\overline{lat}) & 0 & \cos(\overline{lat}) \end{pmatrix} \quad (28)$$

$$R_{\beta} = \begin{pmatrix} 1 & 0 & 0 \\ 0 & \cos(\beta) & \sin(\beta) \\ 0 & -\sin(\beta) & \cos(\beta) \end{pmatrix} \quad (29)$$

$${}^wU^{ecef} = R_{\beta}R_{lat}R_{lon} \quad (30)$$

$${}^w\vec{r}_i = {}^wU^{ecef} {}^{ecef}\vec{r}_i, \quad (31)$$

where \overline{lat} and \overline{lon} are the latitude and longitude corresponding to ${}^{ecef}\bar{\vec{r}}$. With the new position vector in the w frame (${}^w\vec{r}_i$), we calculate the corresponding latitude and longitude in the new frame (wlat_i and wlon_i). The angle β is solved iteratively until the correlation between wlat and wlon is a minimum. We then calculate the probability density function (normal or KDE) with the formulation shown in Equations 15-24 by using wlat_i and wlon_i instead of lat_i and lon_i .

The resulting probability density function obtained from Equation 24 is in the w frame (${}^w\hat{f}$). We can easily express the probability density function in the original frame by doing the following coordinate transformation:

$$\hat{f}(lat_i, lon_i) = {}^w\hat{f}[{}^wlat_i(lat_i, lon_i), {}^wlon_i(lat_i, lon_i)] \cdot |J|, \quad (32)$$

where the determinant of the jacobian matrix, $|J|$, is given by

$$|J| = \frac{\partial {}^wlon_i}{\partial lon_i} \frac{\partial {}^wlat_i}{\partial lat_i} - \frac{\partial {}^wlon_i}{\partial lat_i} \frac{\partial {}^wlat_i}{\partial lon_i}. \quad (33)$$

The new probability density as seen in Figure 3 covers the impact locations a lot better than compared to the unmodified version (see Figure 2).

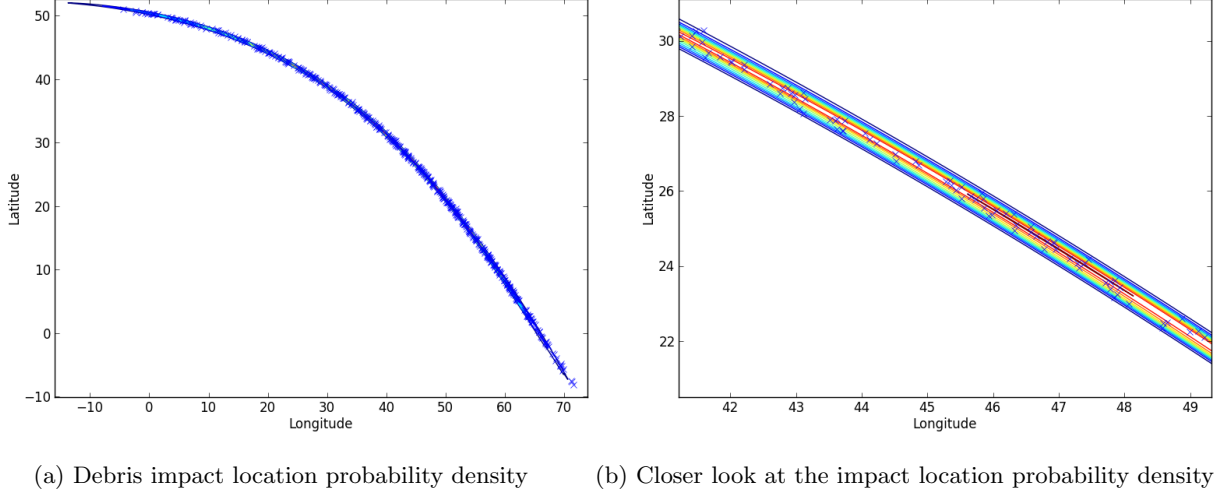


Figure 3: Probability density function results for modified KDE formulation

2. Expected Casualty Formulation

The number of expected casualties, E_c , depends on atmospheric and trajectory parameters. The formulation given here is based on a methodology suggested by the FAA.⁶ The number of expected casualties for people in the open is calculated by:

$$E_c = \sum_{i=1}^{n_d} \sum_{j=1}^{m_d} P_{Iij} E(A_c) \rho_{ij}, \quad (34)$$

where the impact probability of a region P_{Iij} is obtained by integrating the impact probability density over a region of interest. All people inside the casualty area A_c are assumed to be casualties.⁶ The population density for an area at risk ρ_{ij} is obtained from GPW. In general, for people in the open and in different sheltering categories the equation for E_c is shown below:

$$E_c = \sum_{i=1}^{n_d} \sum_{j=1}^{m_d} \left(P_{Iij} \left[\sum_{r=1}^{N_{roofs}} E(A_{C_k}) \rho_{ij} c_r \right] \right), \quad (35)$$

where N_{roofs} corresponds to the number of sheltering categories, c_r is the fraction of people sheltered by the roof type, and the shelter casualty area A_{c_k} depends on the size of the debris and sheltering category.⁹

C. Gas Dispersion

RSAT considers risks due to burning debris emanating toxic gases. There are multiple open source alternatives to model toxic gas dispersion. The most common air dispersion models are plume and puff types. Plume models assume that a plume disperses in the horizontal and vertical directions and follows the wind direction in a straight line. Puff models use discrete puffs emitted from the source, and the path can follow a curved trajectory due to changing winds.

Two software packages currently used by the Environment Protection Agency (EPA) for air dispersion modeling, CALPUFF and AERMOD, were identified to be able to capture some of the physics of toxic gas dispersion for burning debris. CALPUFF is a non-steady puff dispersion model. AERMOD is a plume model, which incorporates air dispersion based on planetary boundary layer turbulence.²⁰ We decided to incorporate AERMOD in the analysis environment due to the relative ease of use and automation.

AERMOD uses two preprocessors AERMAP and AERMET. AERMAP incorporates complex terrain information by using U.S Geological Survey (USGS) digital elevation data. The analysis environment can use AERMAP or assume that there is no complex terrain (terrain elevation set to sea level). AERMET

processes upper air soundings and hourly surface meteorological observations at different locations, which have to be provided as part of the inputs. These observations are ultimately used to determine the wind direction at discrete times.

Burning debris is modeled as area sources. AERMOD only allows changing the rate of gas emission from a source in one hour intervals, thus slightly limiting our modeling capabilities. Toxic debris could be expected to emanate fumes for a few minutes (10-20 minutes); thus we are limited by AERMOD. To work around this issue, we are assuming that all burning debris will emit toxic gases at the same rate for one hour. This leads to the following equation to calculate the emission rate,¹⁹

$$e_{rate} = \frac{m_{gas}}{A_{gas} t_{gas}} \quad (36)$$

where m_{gas} is the amount of toxic gas to be emitted, A_{gas} is the reference area used to model the burning debris as an area source, and t_{gas} is the time for which we expect the gas to burn (1 hour). AERMOD requires the units of e_{rate} to be $\frac{grams}{meters^2 second}$.

The debris propagation module computes the impact location of the burning debris. Once the location is known, a number of receptors around the debris impact location are given as inputs to AERMOD, which then finds the receptors that contain gas amounts exceeding a given threshold. Each receptor has an associated area. The receptors form a cartesian mesh around the impact locations. If a receptor is found to have high gas concentrations, the associated area is considered to be a casualty area. The equation below shows how casualties are calculated,

$$casualties = \sum_{i=1}^{Nr} A_{cg} \rho_i, \quad (37)$$

where A_{cg} is the area associated with the receptor with a gas concentration higher than the threshold i , Nr is the total number of high gas concentration receptors. We repeat the gas dispersion scenario using Monte Carlo, and the average number of casualties (Equation 37) becomes our estimate of E_c .

Effects due to debris landing on water are not modeled. Water is considered to be simple terrain, but population considerations are taken when accessing the population density data.

D. Blast Overpressure

Blast overpressure from a vehicle explosion in midair is an important risk factor to consider during the first few seconds of a launch. An explosive event of this nature is likely to create a blast wave, which could cause peak overpressures that can harm people on the ground. A peak overpressure could damage lungs or rupture eardrums. A blast wave could also harm people inside structures due to flying shards of glass or other elements of the structure.¹⁸ In order to model the peak overpressure effects, we are using the Baker-Strehlow-Tang curves.²¹ Figure 4 shows the relation between the scaled overpressure and the scaled distance. M_f is the flame mach number, and corresponds to the intensity of the overpressure. The scaled distance is calculated by :

$$\bar{R} = \frac{R}{E_t / (p_o)^{1/3}}, \quad (38)$$

where p_o is the ambient pressure, and R is the stand-off distance. The equivalent mass of TNT, m_{TNT} , is calculated by

$$m_{TNT} = \alpha_e m_p E_{mp} / E_{mTNT}, \quad (39)$$

where α_e is the efficiency factor based on energy, m_p is the mass of propellant, E_{mp} is the combustion energy of fuel per unit mass, and E_{mTNT} is the energy per unit mass of TNT.²² Reported efficiency factors can range from 0.1 to 10% with the majority being less than 1 to 2%.²¹ The blast energy E_t is given by

$$E_t = \alpha_e m_p E_{mp}. \quad (40)$$

The scaled overpressure is calculated by

$$\bar{P} = \frac{p - p_o}{p_o}. \quad (41)$$

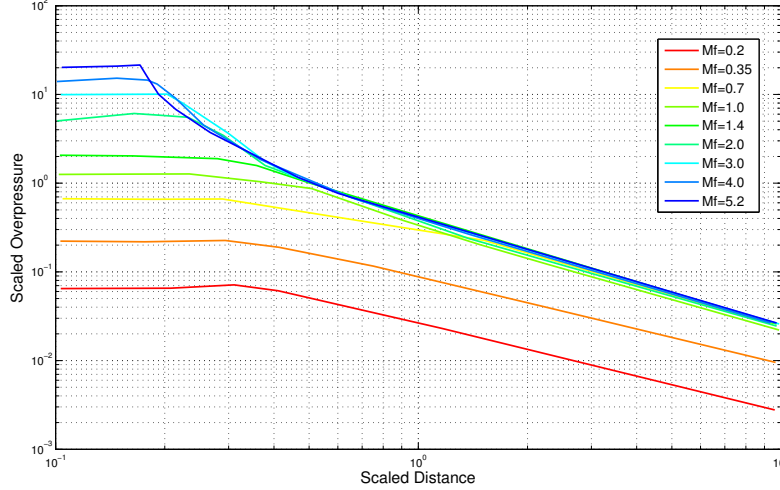


Figure 4: VCE overpressure distributions (Figure from Tang, M.J and Baker, Q.A²¹)

A pressure threshold is selected to ensure that it will cover the peak overpressures that would cause casualties. With the threshold selected, the blast overpressure sphere can be computed to determine if it intersects the Earth's surface. The casualty area is the intersected Earth's surface. All people in that area are considered casualties. To simplify the analysis, all people are assumed to be in the open; thus no flying glass shards or other structural elements can harm people. E_c is given by:

$$E_c = A_{cb}\rho, \quad (42)$$

where A_{cb} is the Earth's surface area that intersects the blast sphere of influence.

E. Explosive Debris

Small explosions could occur in the event of a breakup where some solids such as solid rocket propellant impact the ground at high speeds. For people in the open, we use the same procedure as for the blast overpressure, with the exception that the fraction of TNT is calculated by the Theoretical-Empirical Correlation (TEC) for solid propellant.¹⁸

$$\eta_p = 1.28 \left(1 + \frac{192,000}{W^{0.156}} \left(\frac{S}{V} \right)^{1.55} \right)^{-1}, \quad (43)$$

where W is the propellant weight in pounds, V is the impact velocity in *feet/sec*, and S is the surface hardness factor ($S = 2.92$ for water, $S = 1.81$ for soil, $S = 1.41$ for concrete, and $S = 1$ for steel).¹⁸ The blast energy (Equation 40) is doubled to account for the reflection from the ground. Equation 38 is used to determine the blast casualty area for people in the open. E_c for people in the open is then calculated by using Equation 34 with the updated blast casualty area.

III. Test Cases

A. STS-107 Columbia Accident Simulation

1. Trajectory Calculation

On February 2003, the Space Shuttle Columbia disintegrated during reentry. The breakup of debris from the main vehicle was estimated to have taken about two minutes. Over 80,000 debris pieces were recovered over Texas and Louisiana. The Columbia Accident Investigation Board (CAIB) presented a detailed analysis calculating E_c and risks to aircraft in the vicinity of the debris cloud.⁴ We are using the same debris catalog (see Table 1) as the one used in the CAIB Report.

Table 1: Columbia Accident Debris Groups

Frag Category	Ave. Frag. Wt. (<i>lb</i>)	Ave. Frag. Area (<i>ft</i> ²)	Ballistic Coeff. (<i>lb/ft</i> ²)	No. of Frags
1	0.04	0.143	0.50	1860
2	0.19	0.312	1.00	11260
3	0.22	0.204	1.78	19541
4	0.37	0.185	3.33	13846
5	1.32	0.392	5.60	10901
6	1.77	0.295	10.00	4597
7	2.63	0.247	17.78	6969
8	5.04	0.280	30.00	5387
9	9.67	0.287	56.23	246
10	4.29	0.072	100.00	33
11	800	4.444	300.00	1

There are other input parameters that have not been published, such as the breakup state vectors. Due to the lack of these information, we approximated the last known state vector by finite differencing the last known position vector and by trying to match the simulated impact location of the debris piece having the highest ballistic coefficient ($300\text{lb}/\text{ft}^2$) with the recovered location. The trajectory for the highest ballistic debris piece was used as the reference trajectory of the main vehicle. The reference trajectory was used to obtain the state vectors during a two minute breakup period. The breakup time for each debris piece was simulated as an uniform distribution between 0 and 2 minutes. The state vector at each breakup time was used as the initial condition for propagating all the debris pieces to the ground. We assumed the wind velocity to be $10\text{ft}/\text{sec}$ in the south east direction.

Figure 5 shows the debris location map from the CAIB Report⁴ with our data overlaid for comparison. The results of the impact locations for the simulated pieces of debris agrees with the recovered pieces.

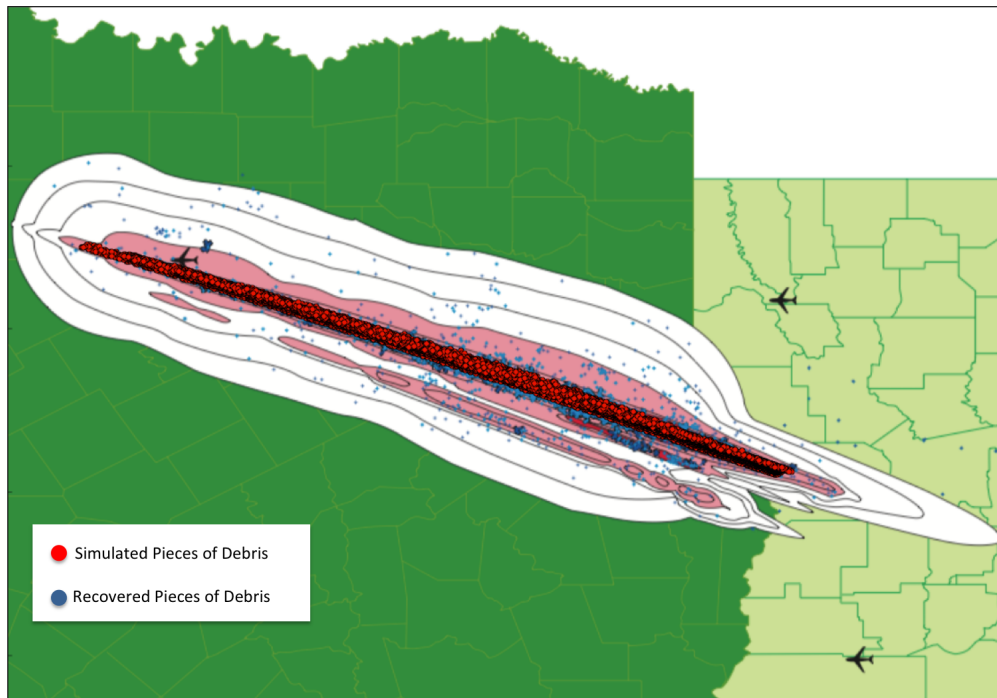


Figure 5: Columbia Accident Debris Locations Comparison (original figure from CAIB Report⁴)

2. E_c Calculation

The next step involves calculating E_c . For this scenario, we used the KDE formulation to calculate the impact probability density function. Sheltering is also taken into consideration, but due to the lack of detailed sheltering information, an average value for the amount of people in the different sheltering categories is used for all population centers (data obtained from CAIB Report⁴). The sheltering distribution used is shown in Table 2.

Table 2: Columbia Sheltering Distribution

Structure Type	Percentage	Structure Type	Percentage
Wood-Roof	39.9	Concrete-Roof	1.5
Wood-1st	3.1	Concrete-1st	1.0
Wood-2nd	0.3	Concrete-2nd	1.1
Steel-Roof	1.4	Tile-Roof	18.1
Steel-1st	0.9	Tile-1st	1.5
Steel-2nd	1.3	Tile-2nd	0.1
Light Metal	3.2	Car	7.1
Composite	0.8	Open	18.7

An important input parameter in computing the probability density function is the number of samples per group (n in Equation 24) to be used in the KDE formulation. Figure 6 shows the convergence study of E_c for 18.7% of people in the open as the number of samples per debris group is increased. The average value of E_c seems to reach convergence at about 5000 samples per group. This large number is due to our assumption that each piece of debris has a different initial state vector.

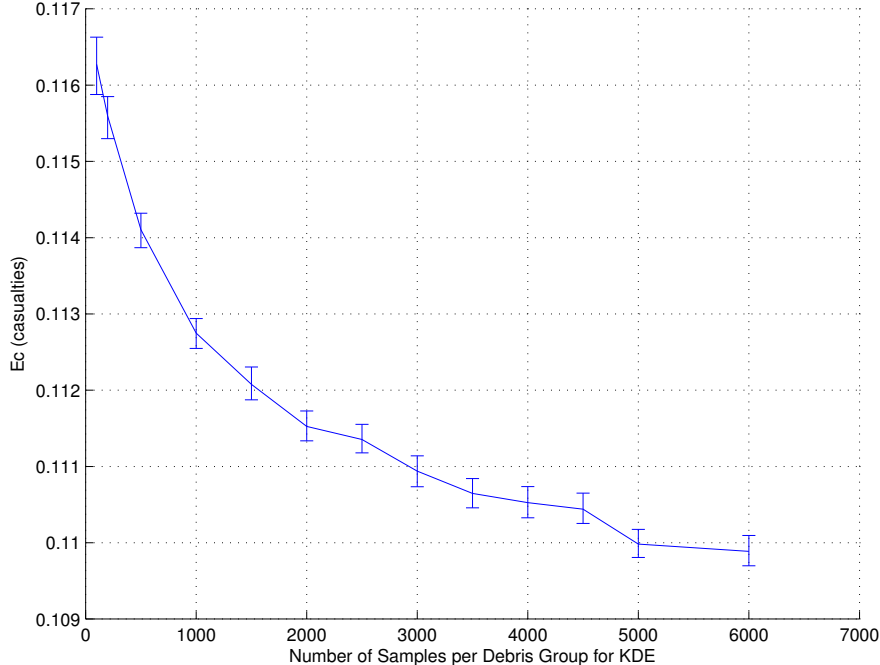


Figure 6: Columbia Accident E_c Convergence

The results are summarized in Table 3. The results are compared with the values reported in the CAIB Report. The differences in the results could be attributed to the fact that we do not use the same set of

assumptions, such as the trajectory, sheltering categories, and population density. Despite these differences, the analysis environment is giving results that are comparable to the CAIB Report.

Table 3: Columbia accident E_c results for 18.7% people in the open

	E_c
CAIB Report	0.14
Simulation	0.11

B. STS-111 Over-flight of Eurasia Simulation

Further validation is performed by considering debris generating scenarios for the STS-111. Stage 2 on-trajectory orbiter failures were modeled at an altitude of 250,000 ft. The failure times studied cover about 490-500 seconds after launch. The same debris catalog as for the Columbia accident simulation is used. The areas that could be affected by a debris generating event are shown in Figure 7.

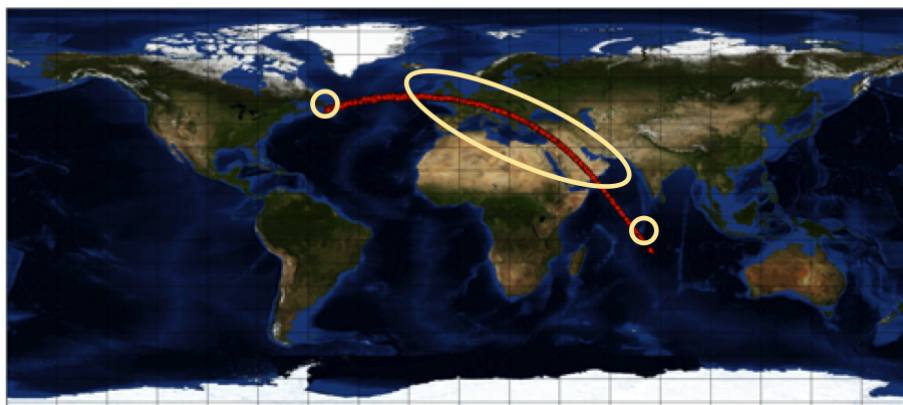


Figure 7: Debris Impact Locations for the STS-111 Simulations

The E_c calculations assumes no sheltering and takes into consideration an orbiter failure rate of $5.85 \times 10^{-6} \text{sec}^{-1}$. Figure 8 shows the mean E_c rate behavior as a function of time, including 99% confidence intervals.

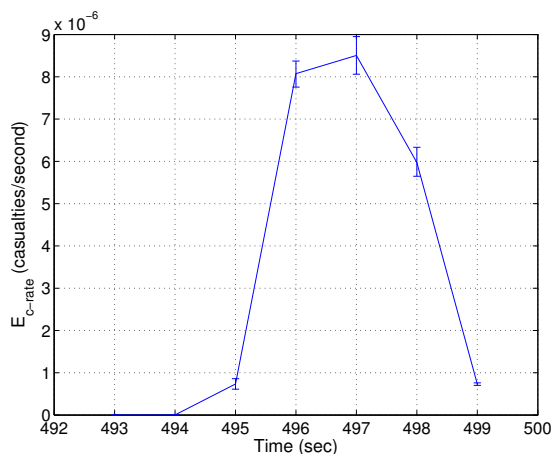


Figure 8: Mean of E_{c_rate} for STS-111 with 99% confidence intervals

Other proprietary studies have reported E_c rate values for this scenario ranging between 2.8×10^{-6} to 4.6×10^{-6} casualties/sec, but it considers sheltering information. Comparing our analysis environment with

other environments is a challenging tasks due to the lack of openly available information for these type of analysis. From this scenario we can see that the analysis environment is showing results within the same order of magnitude as other currently used tools.

C. ELV to ISS Orbit

We developed a safety assessment scenario where the most important pieces of the the safety assesment tool are tested. For this purpose a generic ELV vehicle with characteristics similar to current commercial ELVs was modeled and analyzed. The vehicle has two stages, uses liquid propellant, and is capable of reaching the International Space Station (ISS) orbit. The vehicle's geometry is seen in Figure 9. Aerodynamic databases are computed with Missile Datcom²³ and they become inputs to SPOT to generate an optimal trajectory (Figure 10). This particular mission launches from the Cape to an ISS orbit. The vehicle and mission characteristics are shown in the table below.

Table 4: Vehicle Characteristics

	First Stage	Second Stage
Propellant Mass (kg)	217089	44361
Structurak Mass (kg)	17454	4627
$I_{sp}(s)$	279	342
Max Thrust (N)	500400	445000
Payload Mass (kg)	—	3500

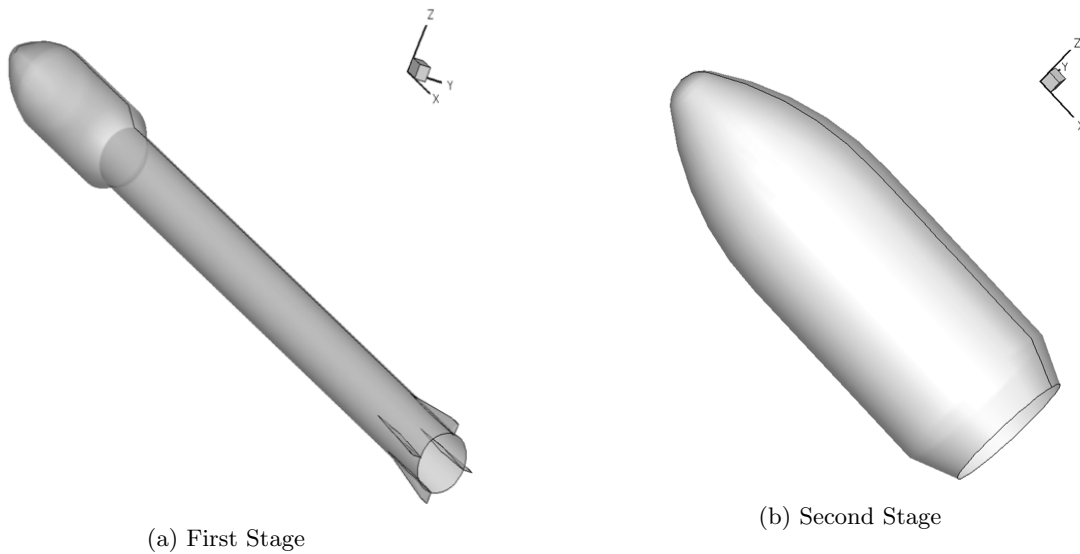


Figure 9: Generic ELV geometry

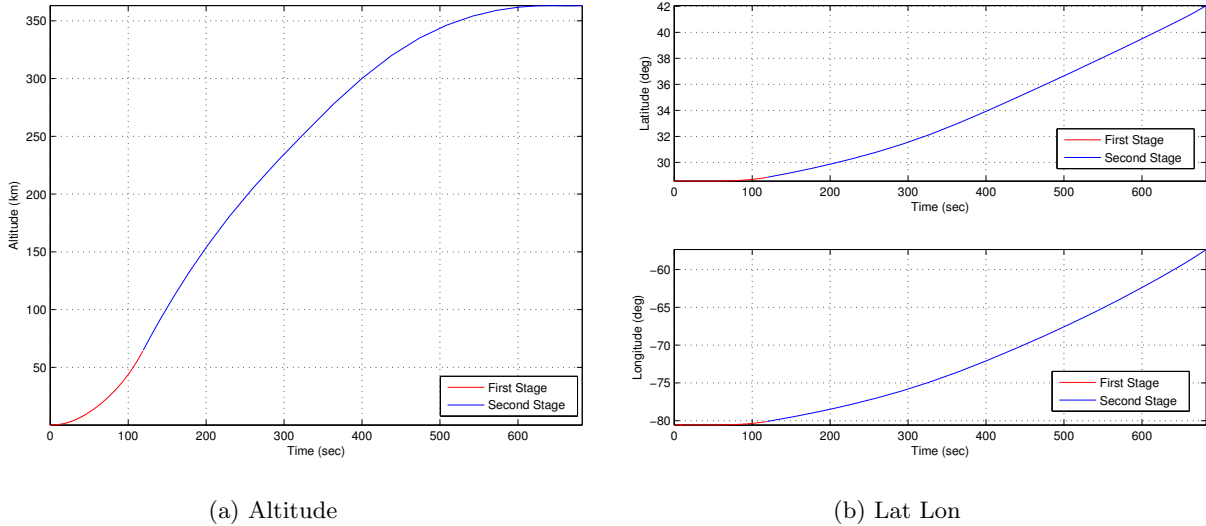
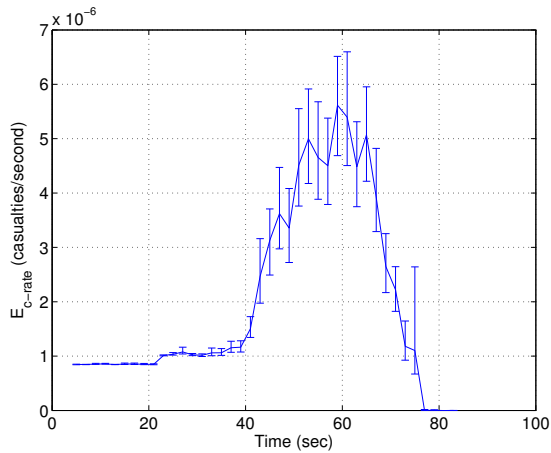


Figure 10: Generic ELV trajectory

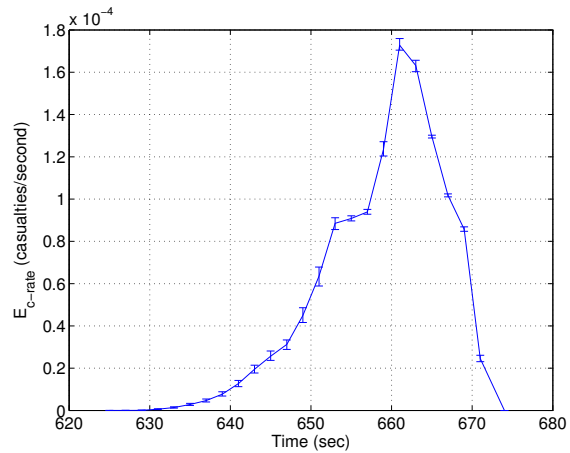
The probability of failure for this vehicle is 0.16, which is the reference value for an ELV with 1 failure in 8 flights.²⁴ Assuming that the failure rate is constant, we approximate the probabilistic failure rate to be $2.286 \times 10^{-4} \text{sec}^{-1}$ for a launch time of 700 seconds. Expected casualty computations for gas dispersion, blast overpressure, and debris propagation are calculated independently.

1. Debris Impact Calculations

The debris catalogs is one of the most important inputs required to calculate the impact locations. Generating debris catalogs for different type of vehicle configurations is a challenge due to the stochastic nature of breakup events. The debris catalogs used for this case are a resized version of debris catalogs developed for the Space Shuttle.²⁵ The resized debris catalogs match the mass of the generic ELV. Figure 11a shows the E_c rate due to pieces of debris impacting the vicinity of the launch pad, while Figure 11b shows the E_c rate for failure times close to the orbit insertion of the vehicle. As in the STS-111 scenario, late in the trajectory the pieces of debris tend to land across Europe and Asia. Explosive pieces of debris are not considered in this case. The debris catalog include number of pieces, reference areas, weights, and aerodynamic coefficients as a function of the freestream mach number. The value for E_{TC} for the debris is 2.8×10^{-3} casualties per flight. The E_{TC} value exceeds the maximum value accepted by the FAA for licensing. More realistic debris catalogs, or adjusted failure rates might yield lower E_{TC} values.



(a) Mean of $E_{c_{rate}}$ with 95% confidence intervals.



(b) Mean of $E_{c_{rate}}$ with 95% confidence intervals.

Figure 11: Inert Debris Casualty Results

2. Gas Dispersion Calculations

Modeling gas dispersion due to toxic pieces of debris requires detailed knowledge of the vehicle in order to determine the characteristics of potential toxic pieces. To test RSAT's gas dispersion modules, we assumed that one of the debris groups (see Table 5) consists of burning pieces of debris that emanate HCl, which is common for solid rocket propellant, but not for liquid propellant as in this example. To calculate the rate of emission we made the conservative assumption that the entire mass of debris will turn into toxic gas and the reference area is used as the area source in AERMOD. Due to modeling limitations in AERMOD, each piece of debris is assumed to emanate toxic fumes for one hour at a constant emission rate. The threshold selected to determine if an area is at risk is a 5 ppm or 7.46 mg/m³ average during a 4 hour window. The threshold value was suggested by the American Conference of Governmental Industrial Hygienist and was previously used in related work.¹⁹

Table 5: Vehicle Characteristics

Number of Pieces	Weight per piece (lb)	Ref Aref (ft ²)	Ball Coeff (lb/ft ²)	Impulse Vel (ft/sec)
2000	64-214	0.69-1.56	116-185	380-490

Figure 12 shows the impact locations of toxic debris, and also the receptors where the toxic levels are above the toxic threshold. The distance between each receptor is 50m which yields a receptor risk area of 2500m². It is clear that the wind direction is heading towards the North East. Some receptors over water contain high toxic levels, this is because there is no special treatment for impacts on water. In most cases, we do not expect this assumption to make a significant difference in the results, because the population density takes care of the casualty calculation over water. The results for the expected casualty rate are shown in Figure 13. The results suggests that gas risks have an effect for about 60 seconds. The E_c values seem to be high because people are assumed to be in the area and without sheltering. Usually people would not be allowed in the vicinity of the launch pad, thus the results should be lower than what is suggested here. The value for E_{TC} for gas dispersion is 1.9 x10⁻³ casualties per flight.

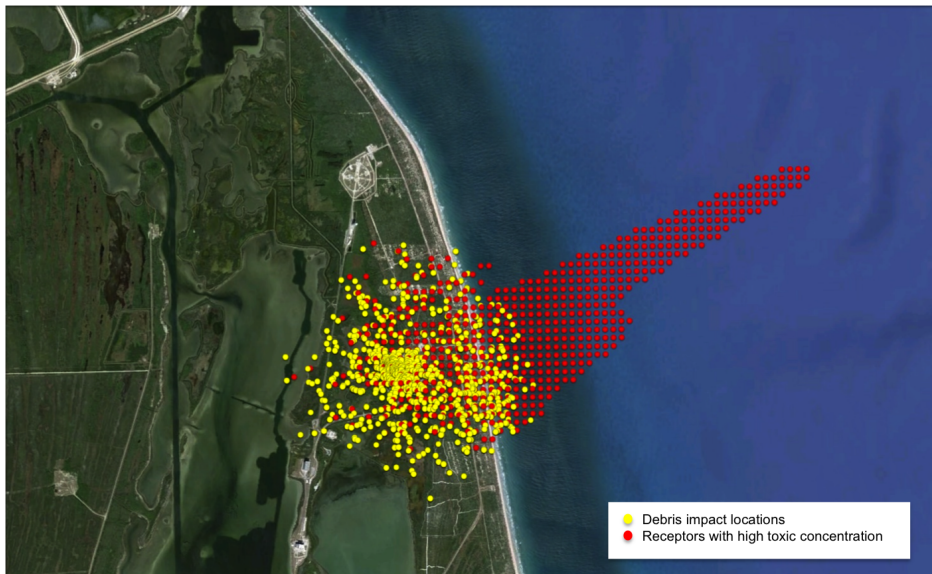


Figure 12: Toxic Debris and Receptor Locations

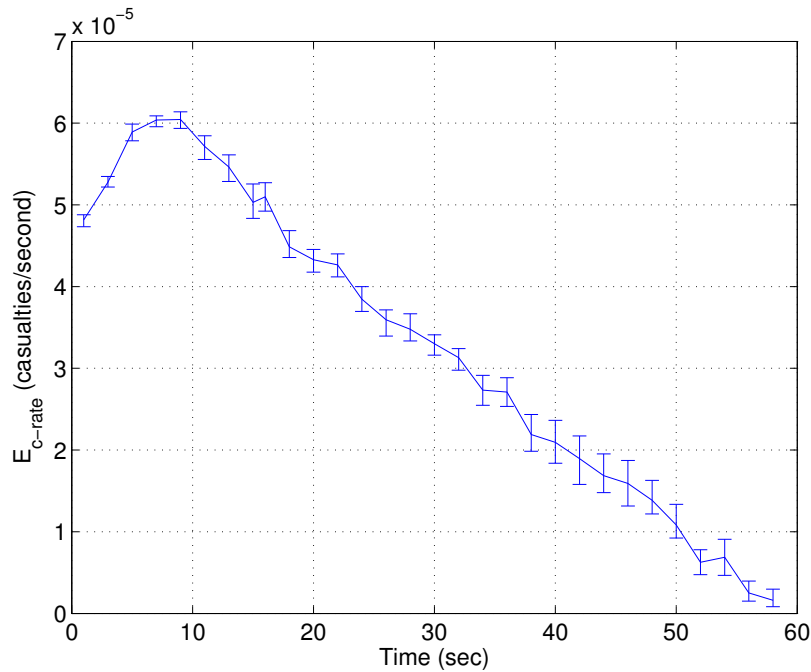


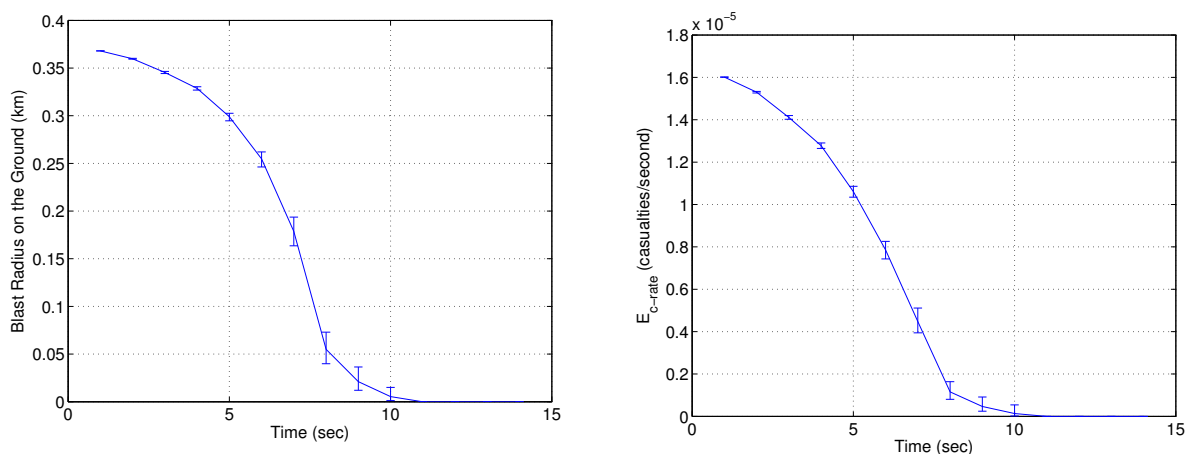
Figure 13: Mean of E_{c-rate} with 95% confidence intervals

3. Blast Overpressure Calculations

Conservative assumptions were made in order to obtain the necessary input parameters. All the propellant (first and second stage) is converted to an equivalent mass of TNT and an α_e of 2% was selected. The range community selects the overpressure threshold based on eardrum protection. A incident overpressure of 2 psi is adopted as the most conservative.²⁶

The blast energy found in Equation 40 is doubled to account for ground effects. Ideally, ground effects should be ignored as the ELV gains altitude, so that the original blast energy equation should be used. To be conservative we decided to assume that the ground affects the overpressure radius at all times (Equation

40 is doubled for the entire trajectory). Results for radius of influence on the ground and E_c rate are shown in Figure 14. The results show that even by doubling the blast energy and considering all people to be in the open, blast overpressure is only a considerable risk the first few seconds after launch. The value for E_{TC} for blast overpressure is 7.49×10^{-5} casualties per flight.



(a) Mean blast radius on the ground with 95% confidence intervals.

(b) Mean of $E_{c_{rate}}$ with 95% confidence intervals.

Figure 14: Blast Overpressure Results

IV. Conclusions and Future Work

This paper demonstrates the use of RSAT to determine the number of casualties on the ground in case of debris generating event during launch or reentry operations. Our analysis of the Columbia accident suggests that RSAT returns comparable results with other tools used to analyze this accident. With this scenario, we were able to evaluate the debris propagation, sheltering, and casualty estimation routines. Validation of blast overpressure and gas dispersion is a bigger challenge due to the lack of published data.

We have demonstrated the use of SPOT to obtain optimal trajectories, and to provide breakup state vectors. The coupling of SPOT with RSAT allows us to create safety assessment scenarios for different missions without heavily depending on proprietary data or tools.

There are other future directions for the work shown here. By identifying the most important models and improving their fidelity, RSAT could provide more confidence in the estimates. RSAT could benefit from improving the blast overpressure to include effects due to structural elements harming people. A better model for gas dispersion, which allows more flexibility of specifying burning rates, would also provide more confidence in the results. Overall, an improvement in the sheltering models for all the modeled risks would most likely have an impact on the confidence of the casualty estimates.

Results from the ELV to an ISS orbit suggest that failures later in the trajectory could lead to considerable casualties. The combination of the trajectory and debris catalogs has an important effect on the final results, further study is necessary to understand what input parameter combinations could lead to the worst case scenario. Also, most ELVs currently operate over non-populated areas. Therefore, it seems that gas dispersion and blast overpressure are only important the first few seconds of the trajectory. Because some potential spaceports would be located in populated areas, the effects of possible accidents over populated areas should be further explored.

Finally, with RSAT already fully automated and able to run thousands of Monte Carlo cases, a rich area of research such as uncertainty quantification is available to us. RSAT could help identify the most important uncertain parameters in the expected casualty calculation, and allow us to quantify how the variance in the inputs affect the variance in the parameters of interest. Understanding these effects will help identify what input parameter combination lead to unacceptable levels of safety.

Acknowledgments

We thank Paul D. Wilde for his guidance in the development of this analysis environment. This work is funded through the Federal Aviation Administration Center of Excellence for Commercial Space Transportation.

References

- ¹Federal Aviation Administration." Office of Commercial Space Transportation. http://www.faa.gov/about/office_org/headquarters_offices/ast/about/,2013.
- ²United States. Department of Transportation. Federal Register. 14 CFR Parts 401, 406, 413, et al. Licensing and Safety Requirements for Launch; Final Rule.
- ³J. B. BAEKER, J. D. COLLINS, and J. M. HABER. "Launch risk analysis", Journal of Spacecraft and Rockets, Vol. 14, No. 12 (1977), pp. 733-738.
- ⁴Appendix D.16. Determination of Debris Risk to the Public Due to the Columbia Breakup During Reentry." Columbia Accident Investigation Board Report. 2003.
- ⁵ACTA." Distant Focusing Overpressure". <http://www.actainc.com/overpressure.html>. retrieved May, 2013.
- ⁶Federal Aviation Administration. Advisory Circular." Expected Casualty Calculations for Commercial Space Launch and Reentry Missions". 2000.
- ⁷"Earth Global Reference Atmospheric Model (Earth-GRAM 2010)." Ionosphere and Thermosphere (Solar and Thermal Environment). http://see.msfc.nasa.gov/tte/model_gram.htm.
- ⁸Center for International Earth Science Information Network (CIESIN). Gridded Population of the World (GPW), Version 3 [online data]. Palisades, NY: CIESIN, Columbia University. Available at <http://sedac.ciesin.columbia.edu/data/collection/gpw-v3>, retrieved June, 2013.
- ⁹Eric W.F Larson, Large Region Population Sheltering Models for Space Debris Risk Analysis. AIAA Atmospheric Flight Mechanics Conference and Exhibit. August 2005.
- ¹⁰Gong, Qi, FaribaFahroo, and Michael Ross. "Spectral Algorithm for Pseudospectral Methods in Optimal Control." Journal of Guidance, Control, and Dynamics. 2008.
- ¹¹Benson, David, and Geoffrey Huntington. "Direct Trajectory Optimization and Costate Estimation via an Orthogonal Collocation Method." Journal of Guidance, Control, and Dynamics. 2006.
- ¹²Fahroo, Fariba, and Michael Ross. "Direct Trajectory Optimization by a Chebyshev Pseudospectral Method." Journal of Guidance, Control, and Dynamics. 25.1 (2002):
- ¹³P. E. Gill, W. Murray, and M. A. Saunders (2005). "SNOPT: An SQP algorithm for large-scale constrained optimization". SIAM Review 47(1), 99-131.
- ¹⁴A. Wchter and L. T. Biegler, On the Implementation of a Primal-Dual Interior Point Filter Line Search Algorithm for Large-Scale Nonlinear Programming, Mathematical Programming 106(1), pp. 25-57, 2006
- ¹⁵Kuhn, H. W, and Tucker, A. W. (1951). "Nonlinear programming". Proceedings of 2nd Berkeley Symposium. Berkeley: University of California Press. 7. W. Karush (1939). Minima of Functions of Several Variables with Inequalities as Side Constraints. M.Sc. Dissertation. Dept. of Mathematics, Univ. of Chicago, Chicago, Illinois.
- ¹⁶Baeker, James, J.R Cavalli, and Mathew Morris. "Downrange Overflight Risk Analysis Methods for Space Shuttle Launches." AIAA Atmospheric Flight Mechanics Conference and Exhibit, No AIAA 2005-6226, San Francisco, CA., August 2005.
- ¹⁷Glonek, Gary, Timothy Staniford, et al. Australian Government. Department of Defence. "Range Safety Application of Kernel Density Estimation". January 2010.
- ¹⁸Federal Aviation Administration. Flight Safety Analysis Handbook Version 1.0. 2011.
- ¹⁹SALA-DIAKANDA, SERGE N. "A Framework for the Assessment and Analysis of Multi-hazards Induced Risk Resulting from Space Vehicles Operations". Diss. University of Central Florida, 2007.
- ²⁰U.S Environmental Protection Agency. "AERMOD IMPLEMENTATION GUIDE. 2009".
- ²¹Tang, M. J. and Baker, Q. A. (1999), A new set of blast curves from vapor cloud explosion. Proc. Safety Prog., 18: 235240. doi: 10.1002/prs.680180412
- ²²C. J. H. van der Bosch, R. A. P. M. Weterings. Methods for the Calculation of Physical Effects: Due to Releases of Hazardous Materials (liquids and Gases) : Yellow Book. 2005.
- ²³Blake, William. "Missile Datcom-1997 Status and Future Plans." AIAA 15th Applied Aerodynamic Conference.
- ²⁴United States. FAA Commercial Space Transportation. "Guide to Probability of Failure Analysis for New Expendable Launch Vehicles". 2005.
- ²⁵National Surface Weapons Center. "Space Shuttle Range Safety Command Destruct System Analysis and Verification: Phase III-Breakup of Space Shuttle Cluster Via Range Safety Command Destruct System." 1981.
- ²⁶Range Safety Group Risk Committee. "Common Risk Criteria Standards for National Test Ranges: Supplement." 2007.